Asian Journal of Geological Research

Volume 7, Issue 1, Page 74-87, 2024; Article no.AJOGER.114779

Application of Aeromagnetic Data to Delineate the Mineralization Zones within Shanga (Sheet 96) Northwest Nigeria

Akpaneno, A. F. [a*] and Tawey, M. D [b]

[a] Department of Geophysics, Federal University Dutsinma, Katsina, Nigeria.
[b] National Water Resources Institute, Mando Road, Kaduna, Nigeria.

Authors' contributions

This work was carried out in collaboration between both authors. Both authors read and approved the final manuscript.

Article Information

Open Peer Review History:
This journal follows the Advanced Open Peer Review policy. Identity of the Reviewers, Editor(s) and additional Reviewers, peer review comments, different versions of the manuscript, comments of the editors, etc are available here: https://www.sdiarticle5.com/review-history/114779

Original Research Article

Received: 24/01/2024
Accepted: 26/03/2024
Published: 01/04/2024

ABSTRACT

The goal of the present study is to identify and delineate the mineralization zones and depths of prospective mineral occurrences in Shanga (sheet 96), parts of the northwest Nigerian basement complex, by analyzing aeromagnetic data. This was accomplished by reducing the residual magnetic intensity (RMI) data for the research area to the equator (RTE), which was followed by the application of two source edge detection/interpretation techniques; first and second vertical derivatives (FVD and SVD), while the analytic signal (AS), was applied to the TMI data. The AS approach of depth estimation was also applied to the Shanga RMI data to establish the minimum depth at which the minerals are likely to occur. Using FVD map, structures that may be responsible for mineralization within the study area were identified and confirmed to eastern basement portion of the study area. The primary structural trend in the region is ENE-WSW, followed by NE-SW, WNW-ESE, NW-SE, and NNE-SSW. The high analytic signal within the schist has been attributed to intrusions and solidification of mineralization fluids with structural linkages, allowing the area's

**Corresponding author: Email: aniefiokakpaneno@gmail.com;*

mineralization zones to be identified. The analytic signal map showed amplitudes ranging from 0.001 nT/m to 0.421 nT/m. Additionally, the SVD map showed mineralization boundaries that matched the AS map's mineralization zones. The analytic signal depth method revealed a minimum depth of occurrence for the minerals ranging from 0 to 11.457 m, and the mineralization zones delineated have one or more structural lineaments passing through them, confirming that they are responsible for mineralization fluid passage and mineralization hosting within the study area.

Keywords: Depth; mineralization; AS; FVD and SVD.

1. INTRODUCTION

Nigerian mineralization is dependent on the geology and rock structure [1], (Kearey et al*.* 2002); [2,3] and to identify prospective rock types and lineaments that serve as conduits for mineralization fluids during magmatic events and serve as hosts for most solid minerals, the recently acquired high-resolution airborne potential data may offer a solution [4]. Its application in mineral exploration, especially around hydrothermal alteration prospects, is to accentuate the structural regime in the region to define suitable pathways that may have supported hydrothermal fluid circulation systems relevant to mineral accumulation [2,5,6,7,8]. The current study region lies in the north-western Nigerian basement complex, which is made up of the migmatite gneiss complex and the schist belts and is partially to the west of the sedimentary Sokoto basin. Most of the country's solid minerals, according to historical accounts, can be found within the western half of Nigeria or in the nation's schist belts (Fig. 1). Reconnaissance surveys are necessary in any geophysical fieldwork including solid mineral exploration and the present study is motivated by the fact that structures typically play a key role in mineralization studies. Since geophysical methods are essential in characterizing geological features including faults, folds, shear zones, and other favorable places for mineralization, they are widely used globally as fundamental tools for geological interpretations [9], Mohamed et al*.* 2019 [10].

Numerous studies have been conducted within the schist belts region that describe the hydrothermally altered zones which historically, have hosted most solid minerals in Nigeria especially gold [11,12,13,14,15,16,17,18,19,20, 21,22]. Since the purpose of the work is to identify mineralization zones and determine the depth at which mineralization may occur within the research area, the Roest et al*.* [23] analytic signal magnetic source locating technique was applied to identify magnetic sources there. Additionally, derivatives (first and second vertical derivatives) are typically very effective tools for structural delineation (fault, joints, and fractures) and delineation of source boundaries [24]. These tools were also applied to the magnetic data of the region for structural and boundary of source delineation with their depth of occurrence using the analytic signal depth method as proposed by Roest et al*.* [23] to delineate the source boundaries.

1.1 Location and Topography of the Study Area

The study area is in north-western portion of Nigeria, bordering Niger and Kebbi states, with boundaries that range from longitudes 4^0 30' east to longitudes 5^0 00' east and latitudes 11^0 00' north to latitudes 11^0 30' north (Fig. 1). The research area is somewhat outcropping Basement [25,26], and sedimentary cover (part of Iullemeden Basin) with topography that ranges from 132 m for low elevated portions around south-western part of the area (Koko, Tungan Magaje, Shanga, Dugu Tofo Ganwo and Nasarawa) to 352 m for extremely high elevated parts particularly regions north to south of Dakku town as gotten from interpretation of Digital Elevation Model (DEM) Shuttle Radar Topography Mission (SRTM) of the study region (Fig. 2).

1.2 Tectonic Settings and Geology of the Study Area

The research region is located south of the Tuareg Shield, between the West African and Congo Cratons, and is also a component of the Nigerian basement complex, which is tectonically a part of the Pan-African mobile belt [27]. It has been intruded by the Mesozoic calc-alkaline ring complexes (Young Granites) of the Jos Plateau, and Cretaceous and newer sediments are unevenly overlaid. The Liberian (2,700 Ma), Eburnean (2,000 Ma), Kibaran (1,100 Ma), and Pan-African cycles of deformation, metamorphism, and remobilization are believed

to have produced at least four major orogenic cycles that produced the basement rocks (600 Ma). Extreme deformation, isoclinal folding, regional metamorphism, and significant migmatisation were all present in the first three stages, which were also associated with these processes. Syntectonic granites and homogenous gneisses were produced as a result of broad migmatisation, regional metamorphism, and granitization and gneissification that followed the Pan-African deformation [28]. Extreme deformation, isoclinal folding, regional metamorphism, and significant migmatisation were all present in the first three stages, which were also associated with these processes. The final stages of this last deformation were followed by the late tectonic placement of granites and granodiorites, as well as related contact metamorphism. Faulting and fracture marked the end of the orogeny [29,30]. The Pan-African Orogeny is thought to have produced the structures in the study area.

Fine-grained biotite granite, medium-grained biotite granite, River Alluvium, biotite gneiss, Augene gneiss, undifferentiated schist including phyllites, quartzite and quartz schists, quartz and mica schists, sandstones, siltstones, and clays, as well as migmatitic granite gneiss and migmatite, are among the rocks in this area (Fig. 3).

This analysis's aeromagnetic data came from the Nigerian Geological Survey Agency (NGSA) [31]. The high-resolution airborne data were gathered by Fugro Airborne Surveys. The survey was conducted in 2009 along a series of NW-SE flight lines of magnetic surveys flown at 500 m line spacing and 80 m terrain clearance.

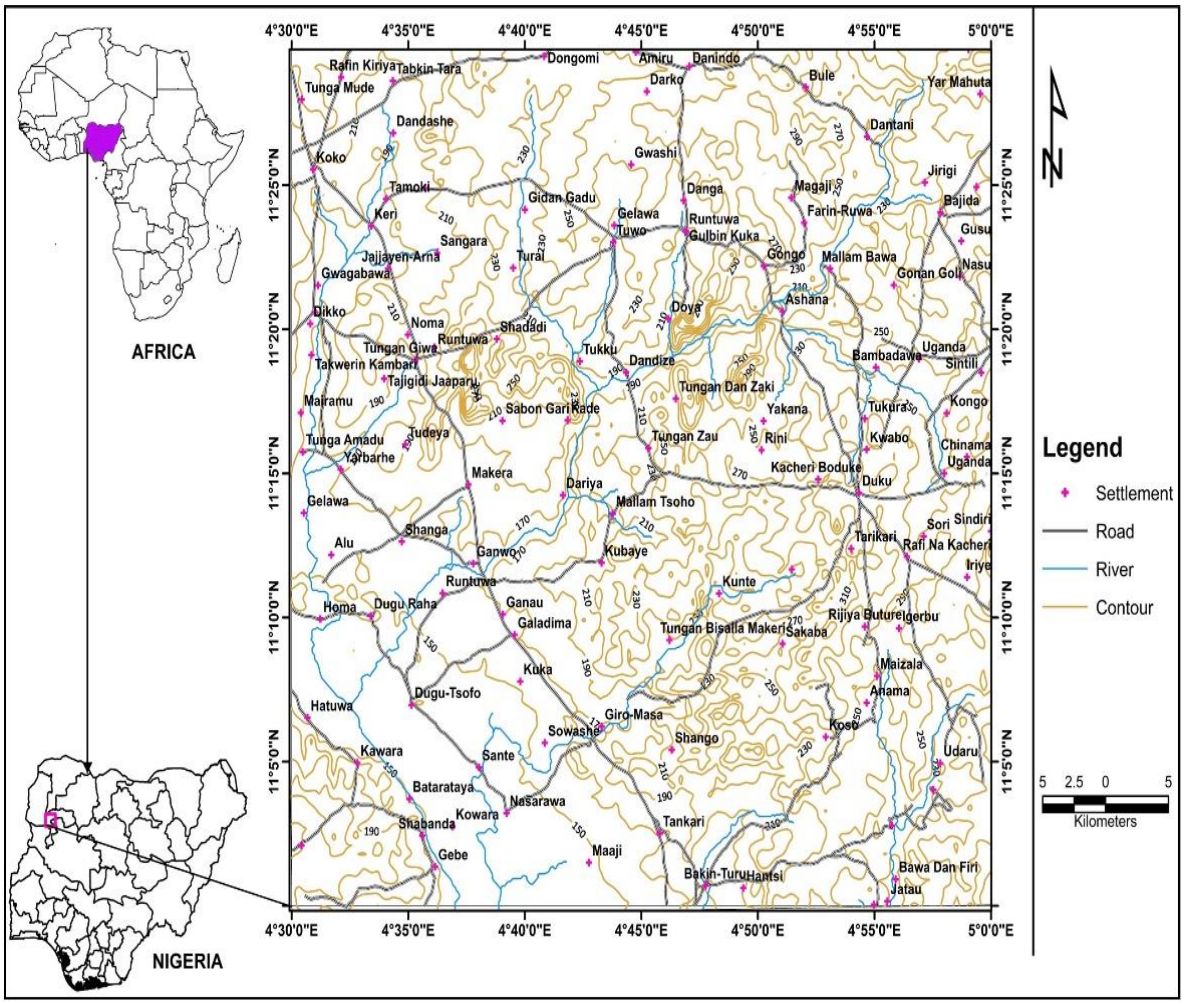

Fig. 1. Location map of the study area (Adapted from Tawey et al., 2023a)

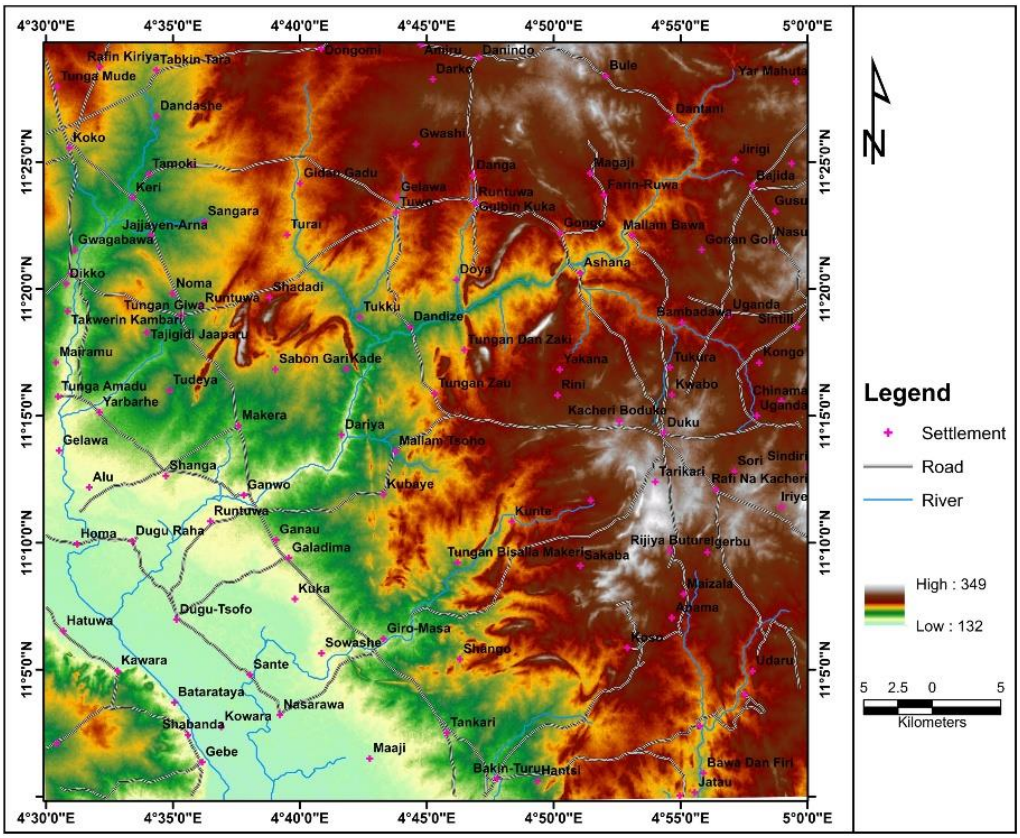

Fig. 2. Digital Elevation Model (DEM) of the area

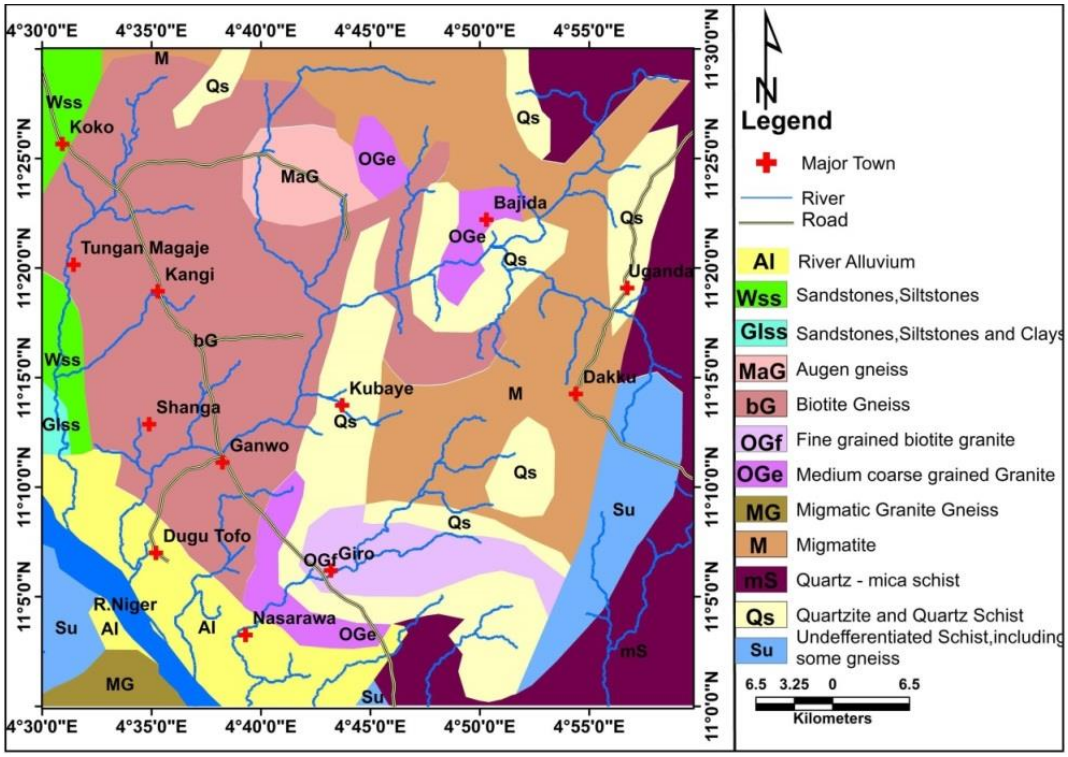

Fig. 3. Geologic map of the area (Adapted from Tawey et al. [5])
Source of Aeromagnetic Data

2. METHODOLOGIES

Total magnetic intensity data (TMI) of the research area were first separated into regional and residual data since the former are from shallow sources and the latter are from deeper sources. The residual magnetic intensity data (RMI) was reduced to the magnetic equator (RTE) using Oasis Montaj version 8.3. The RTE data was subjected to the first vertical derivative (FVD) filter to produce the FVD grid, which was then saved as a map. The map was then exported into Arc Map version 10.5 environments to manually delineate the structures within the study area. Additionally, the TMI data was subjected to the Analytic signal (AS) filter to create the analytic signal grid, which was also exported as a map. This map showed the boundaries of high magnetic zones that were identified as potential zones for mineralization and are places of interest for mineralization.

The border of the high magnetic source, which was delineated using the analytic signal approach as well as mapped structures, was also delineated using the second vertical derivative filter (SVD) applied to the RMI data reduced to the equator (RTE). The borders of the sources and the depth of the mineral occurrences were assessed using the analytic signal approach, and the structures defined from the FVD map were superimposed on both the AS and SVD maps to determine the coincidence of the structures drawn to source locations.

2.1 Theory of Methods

2.1.1 Reduction to the Magnetic Equator (RTE)

With the assumption that all magnetic fields seen in the study region are the result of induced magnetic effects, the application of the RTE technique is to create a magnetic map equivalent to what would have been obtained if the area had been surveyed at the magnetic equator. Data that was collected while the earth's magnetic field was inclined is transformed into data that would have been collected while the magnetic field was vertical by this filter. Anomalies are centered over portions where their sources are located using this technique at low magnetic latitudes. This technique can simplify data interpretation without sacrificing its geophysical significance. We use the equation below for RTE transformation.

$$L(\theta)=\frac{[\sin(I)-i.\cos(I).\cos(D-\theta)]^2 X(-\cos^2(D-\theta))}{[\sin^2(I_a)+\cos^2(I_a).\cos^2(D-\theta)]X[\sin^2(I)+\cos^2(I).\cos^2(D-\theta)]}\ \text{if}(\backslash I_a \backslash)<(\backslash I \backslash), I_a=1 \quad (1)$$

Where I represent the geomagnetic inclination, I_a is the inclination for amplitude correction, *D* represents the geomagnetic declination, Sin (*I*) is the amplitude component while *i*Cos(*I*)Cos(D-θ) is the phase component given by Holden et al*.* [32] and Core et al*.* [33].

2.1.2 Vertical derivatives

Vertical derivative vertical gradient filters accentuate short-wavelength components of the field at the expense of longer wavelengths [24]. Vertical derivative filters are generally applied to gridded data using FFT (Fast Fourier Transform) filters. Various vertical derivatives of the magnetic field can be computed by multiplying the amplitude spectra of the field by a factor of the form:

$$\frac{1}{n}\left[(U^2+V^2)^{\frac{1}{2}}\right]^n \quad (2)$$

where n is the order of the vertical derivative, and (U, V) is the wavenumber corresponding to the (x, y) directions respectively.

2.1.3 Analytic signal method (AS)

The AS allows for the analysis of low-latitude magnetic fields without the worries of the RTP operator since it is less sensitive to the inclination of the geomagnetic field than the original TMI data. Gradient enhancement is a technique for AS that is connected to magnetic fields using derivatives. Roest et al*.* [23] demonstrated that the expression may be used to calculate the magnitude of the AS from the three orthogonal gradients of the total magnetic field:

$$|A(X,Y)|=\sqrt{\left(\frac{\delta T}{\delta x}\right)^2+\left(\frac{\partial T}{\partial y}\right)^2+\left(\frac{\delta T}{\delta z}\right)^2} \quad (3)$$

where A (x, y) is the amplitude of the analytic signal at (x, y) and T is the observed magnetic anomaly at (x, y).

The depths of the magnetic sources are estimated under the assumption that the anomalies are in two dimensions (2-D). Hence, the depths of the magnetic source anomalies are estimated as given in the equation below:

$$AS1=\sqrt{\left(\frac{\delta fv}{\delta x}\right)^2+\left(\frac{\partial fv}{\partial y}\right)^2+\left(\frac{\delta fv}{\delta z}\right)^2} \quad (4)$$

$$D = \frac{AS}{AS1} * N \quad (5)$$

where, fv = First vertical derivative of the residual map, D = Depth to the magnetic sources, AS = Analytic signal of the residual grid, AS1= Analytic signal of the first vertical derivative of the residual grid.

N = 1 (contact), N = 2 (dike), N = 3 (pipe), and N = 4 (sphere) [34]

3. RESULTS AND DISCUSSION

3.1 The Total Magnetic Intensity (TMI), Residual Magnetic Intensity and (RMI) and Residual Magnetic Intensity Reduced to the Equator (RTE) Maps

Fig. 4a represents the total magnetic intensity map while Fig. 4b represents the residual magnetic intensity map of the study area. From Fig. 4a, the susceptibility varies between 33000.7 nT low to 33200.5 nT high. High values are confined to the southwestern portion of the map while low areas are confined to the northwest and southeastern portion of the map with alternating occurrences of magnetic lows and highs which are attributed to the presence of structure (joints and faults), [5]. In Fig. 4b, the residual magnetic intensity values vary from -51.862 nT low to 155.432 nT high. Anomaly trends in northeast to southwest and northwest to southeast within the study area. Fig. 5 represents the RMI map reduced to the magnetic equator (RTE), comparing this map to the RMI map (Fig. 4b), the difference between them is very clear in terms of magnetic susceptibility. The magnetic anomaly ranges from 148.362 nT low to 47.620 nT high on the RTE map as compared to the RMI map where it is -51.862 nT low to 155.432 nT high.

Comparing the RTE map with the geologic map (Fig. 3), it is visible that areas with alternating occurrence of low and high intensity are basement portions with structures concealed beneath the subsurface [5] while the southwest with smooth anomaly trend is the basement portion of the study area.

3.2 The First Vertical Derivative (FVD) map calculated from the RTE

Derivative filters can be applied on aeromagnetic data to enhance weak signal responses and determine the position of deeply buried sources, borders, and structural lineaments [23]. The FVD approach has been utilized to map structures (Fault, fold, and joints) because of its ability to reveal discontinuities in signal responses. Fig. 6a, which represents the FVD map of the study area, showed the western part of the map to be devoid of short wavelength anomalies, which are characterized by sedimentary zones or regions with thick sedimentary cover. Fig. 6b is the FVD map with a structure that has been mapped out. There is no structural lineament in the regions of Koko, Tunga Maje, Shanga, Ganwo, Dugu Tofo,

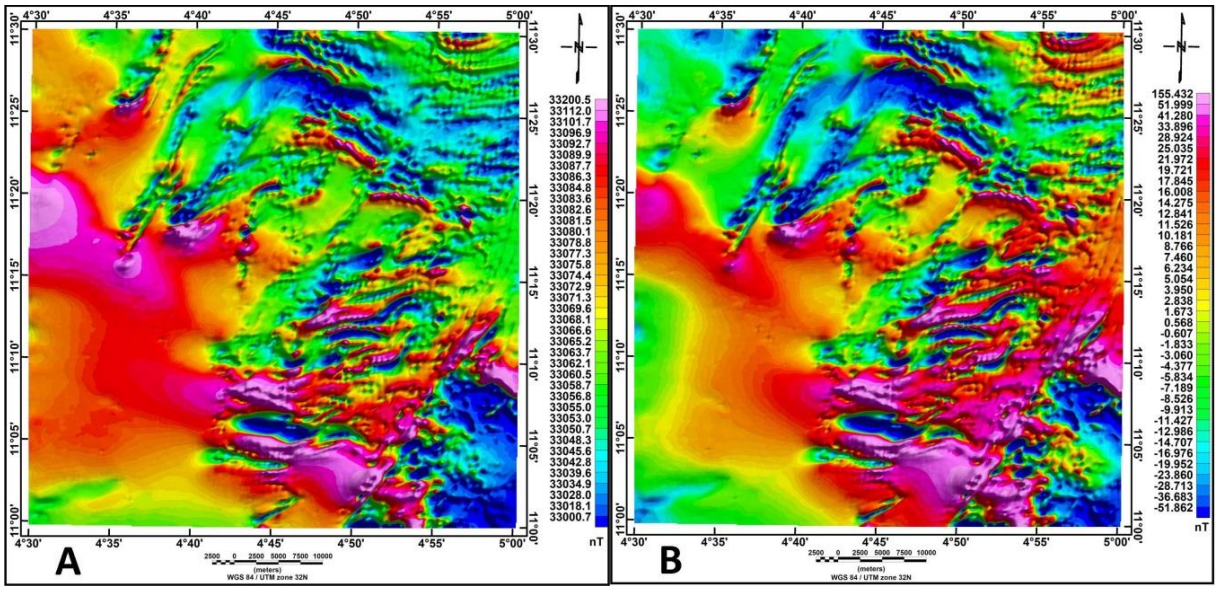

Fig. 4a. TMI map and b. RMI map

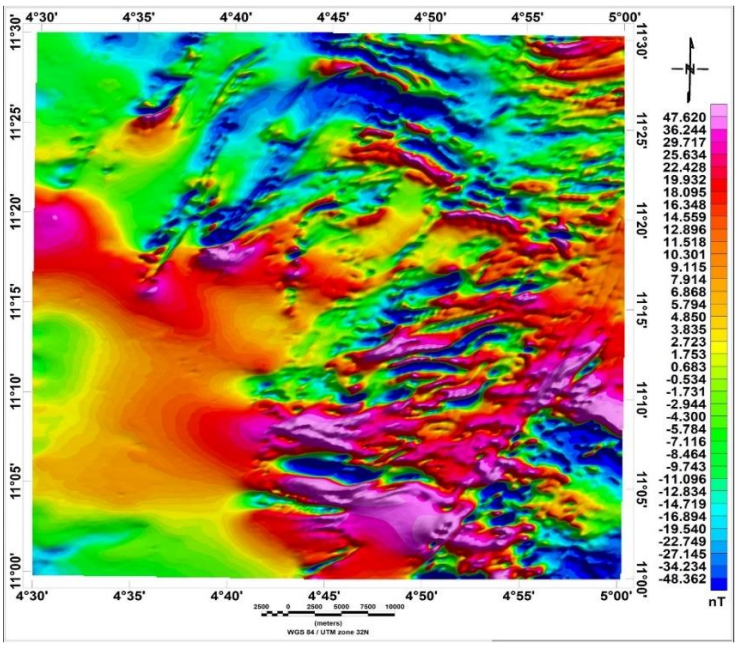

Fig. 5. RTE map of the study area

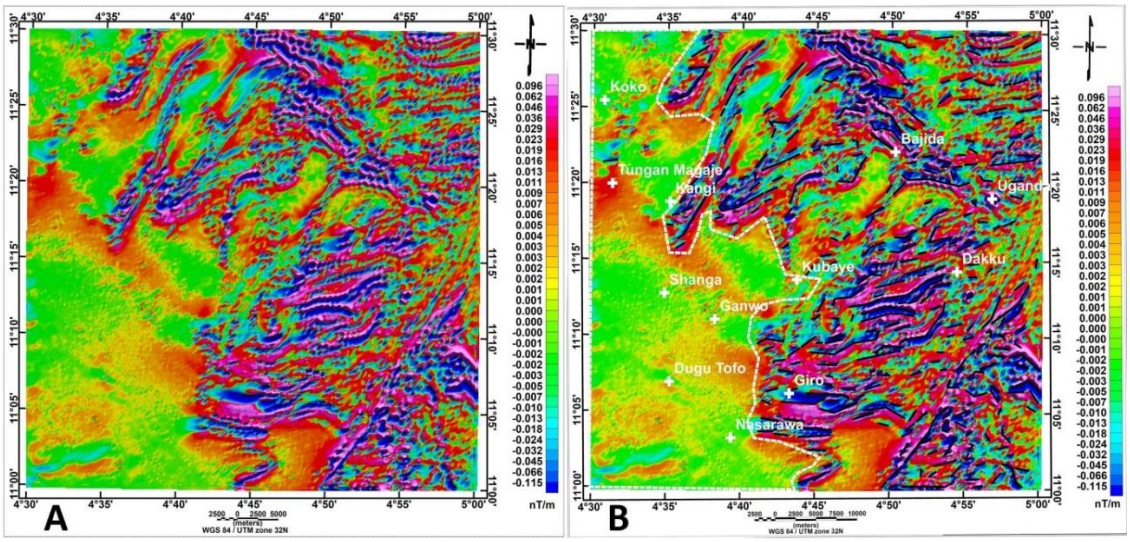

Fig. 6a. FVD Map and b. FVD with Structures

and Nasarawa. Within the area around Bajida and Uganda in the north-eastern part of the map, Dakku around the east, and Giro in the south-central part of the research area, structures were observed and delineated. Fig. 7a is a the FVD structural map while, Rose diagram (Fig. 7b), which represents a succession of tectonic activity that must have influenced the Nigerian basement complex where the current study area is located, was created using these manually outlined structures as shown in Fig. 7a. Statistical trend analysis has revealed that the ENE-WSW trends are the most prevalent, followed by NE-SW, WNW-ESE, NW-SE, and NNE-SSW trends (Fig. 7b).

3.3 The Analytic Signal Map

The AS filter applied to the TMI data helped to reduce the influence of remanent magnetization caused by magnetic inclination or declination. This was done to emphasise the borders of magnetised entities and form peaks over smaller causative bodies [23]. This approach can effectively demonstrate the amplitude magnitude of structural characteristics depending on their

magnetization response since the peaks of the magnetised bodies are cantered symmetrically over their sources through a shape transformation that only depends on the magnetization strength and direction concerning the magnetization vector [35]. Fig. 7a depicts the research areas AS map, and Fig. 7b depicts the geology of the study area on the analytic signal map. In Fig. 7a, the amplitude of the AS map varies from 0.001 nT/m low to 0.421 high. Low analytic signal is observed at the west of the research area confirming that the geology (sedimentary) of the portion. The basement portion withing this area with low AS is a portion of the basement complex with thick sedimentary cover. The rock type present may be the cause of the increased in AS amplitude to the east of the research region (Schists with Granitic intrusions). The geology of the area overlaid on the AS map shows that mineralization will be very high within the schist and other rocks in this location. Also, intrusions and solidification of mineralization fluids may be responsible for the significant AS found within the schist. Therefore, the potential mineralization zones are those with high analytic signal.

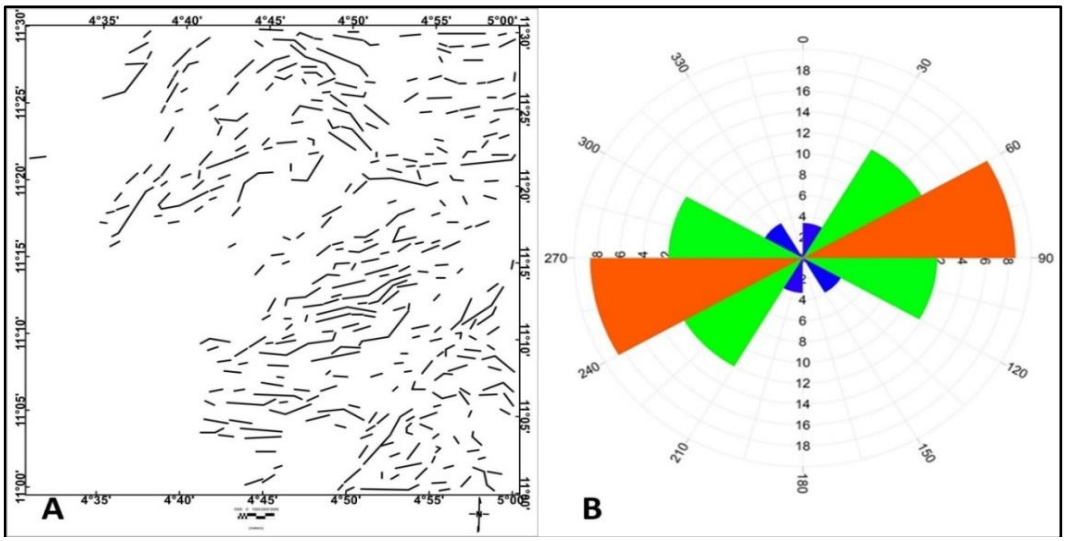

Fig. 7a. Structures from FVD Map b. Rose Diagram from FVD Structures

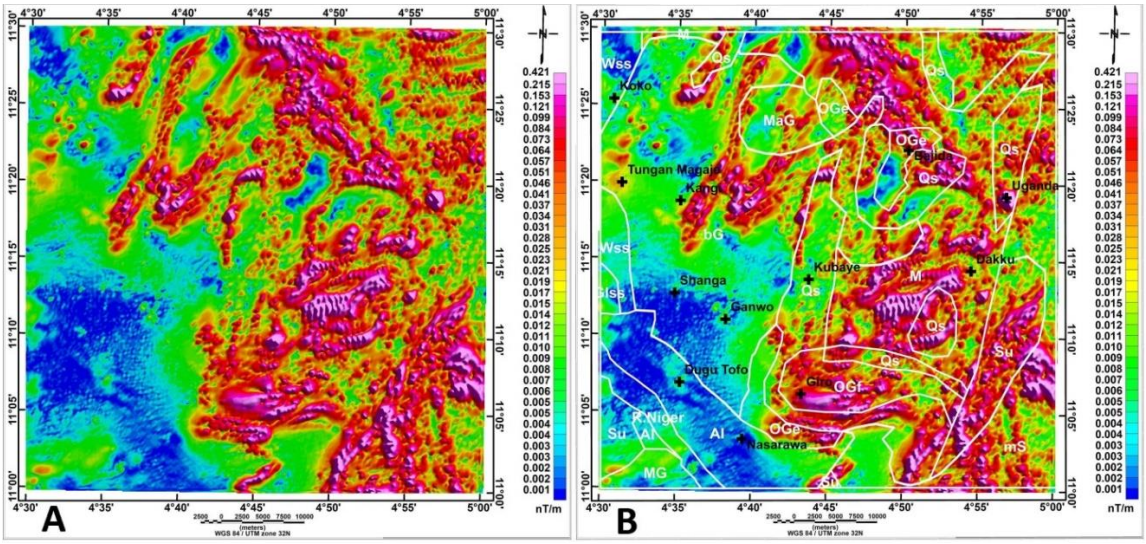

Fig. 8a. Analytic Signal Map and b. Analytic Signal Map with Geology

OGf = fined grained biotite granite, OGe = medium-grained biotite granite, R= River Alluvium, bG = biotite gneiss, MaG = Augene gneiss, Su = undifferentiated Schist including phyllites, Qs = Quartzite and Quartz schists, mS = Quartz and mica schists, sandstones, GIss = siltstones and clays, Wss = sandstones and siltstones and MG = Migmatitic granite gneiss and M = Migmatite

The AS map was overlaid with the structures identified by the FVD map (Fig. 6a) (Fig. 9a) and the structures are observed to fall directly on portions with high analytic signals which imply that these structures are channels through which mineralisation fluids intruded into other rocks within the study area and this has made it possible for the prospective mineralisation zones within the study area to be delineated using white polygons (Fig. 9b).

3.4 The second Vertical Derivative Map (SVD)

Fig. 10a represents the SVD map of the study area while Figure 10b represents the SVD map with structures that were delineated, overlaid on it with anomaly boundaries also delineated using white polygons just like the case of the AS map (Fig. 8b). The SVD map also revealed the boundary between the sedimentary portion and the basement portion of the study area. On comparing the mineralisation zones delineated using the SVD and the AS methods (Figs. 11a & 11b), it is observed that the two methods have aided in the characterization of the lithology of the study area to be either basement or sedimentary on a general geological classification. Also, mineralisation boundaries delineated on the SVD map coincided with the areas of high analytic signal delineated using the analytic signal method. The delineated mineralisation zones have been overlaid on the geologic map of the study area with the structural

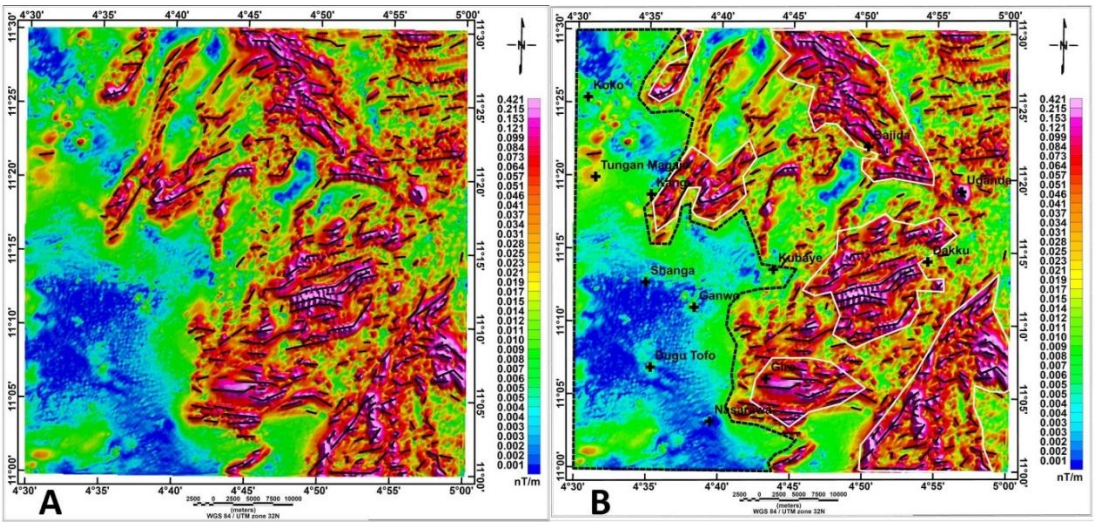

Fig. 9a. AS Map with Structures and b. AS Map structures and Mineralization zones boundaries

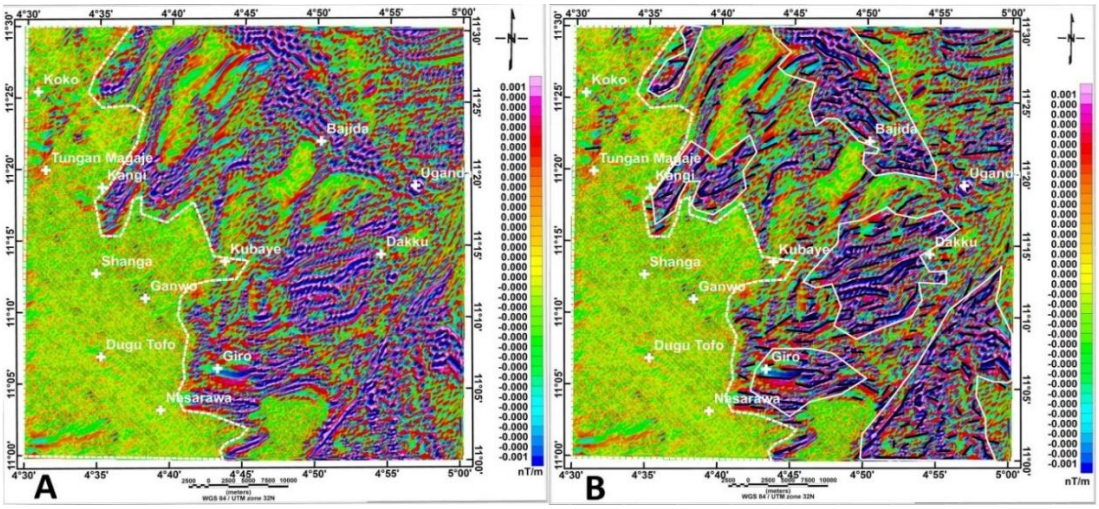

Fig. 10a. Second vertical Derivative map (SVD) Map and b. Second Vertical Derivative (SVD) with Structures and mineralization zone boundary

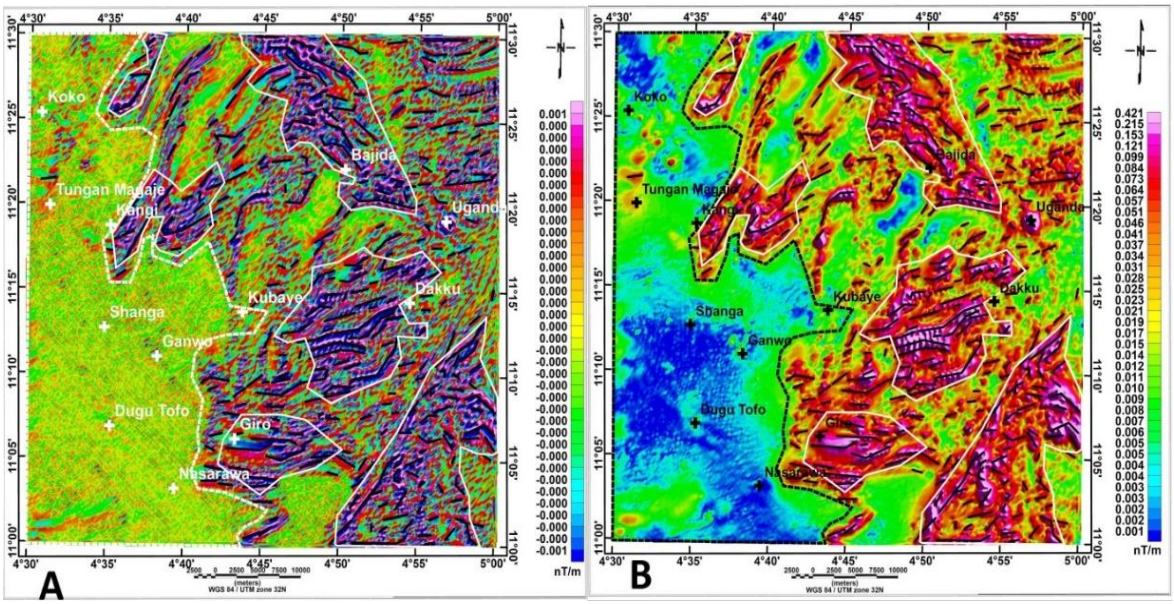

Fig. 11a. Second Vertical Derivative (SVD) with mineralization zone boundary and b. Analytic signal with mineralization zones

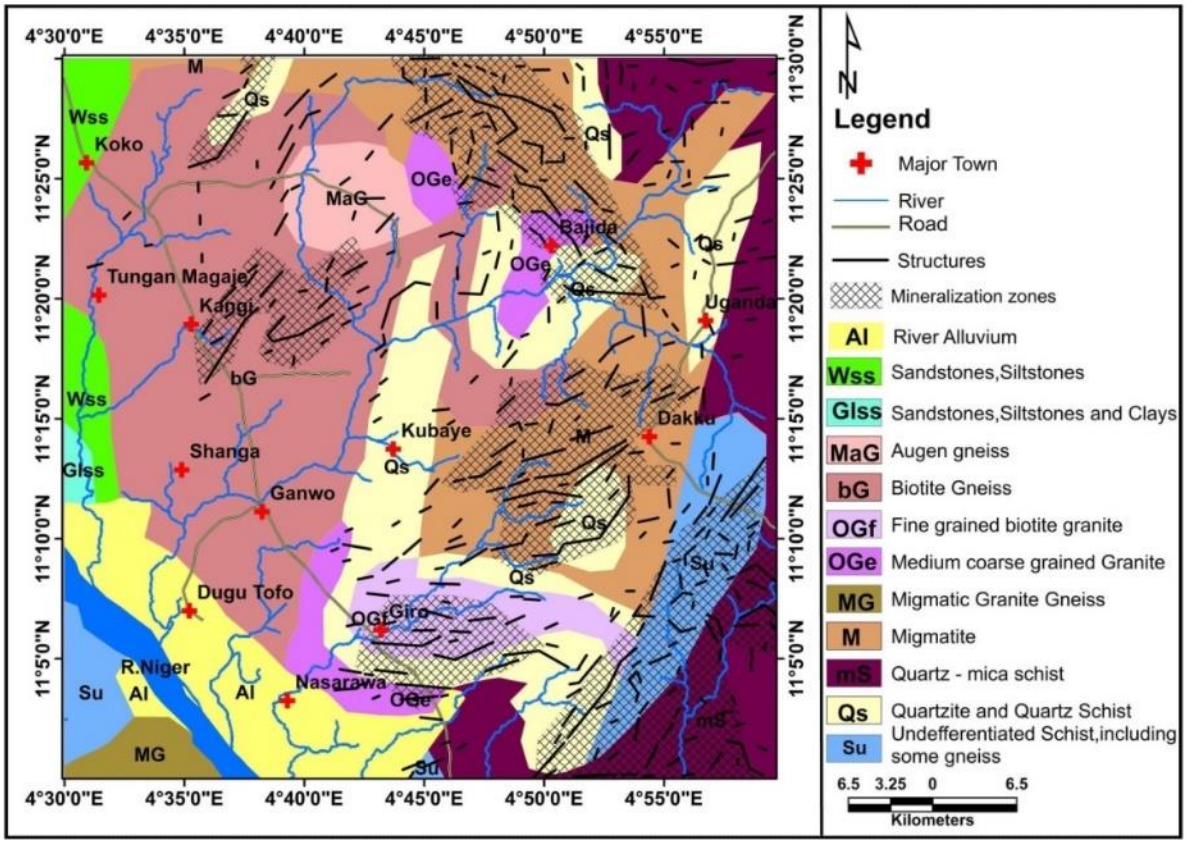

Fig. 12. Integration of Shanga Structures with the Geology (NGSA, 2009)

lineaments (Fig. 12) bearing in mind that structures are conduits and hosts for mineralization. Each mineralization zones delineated have one or more structural associations which confirm that structures control mineralisation within the study area.

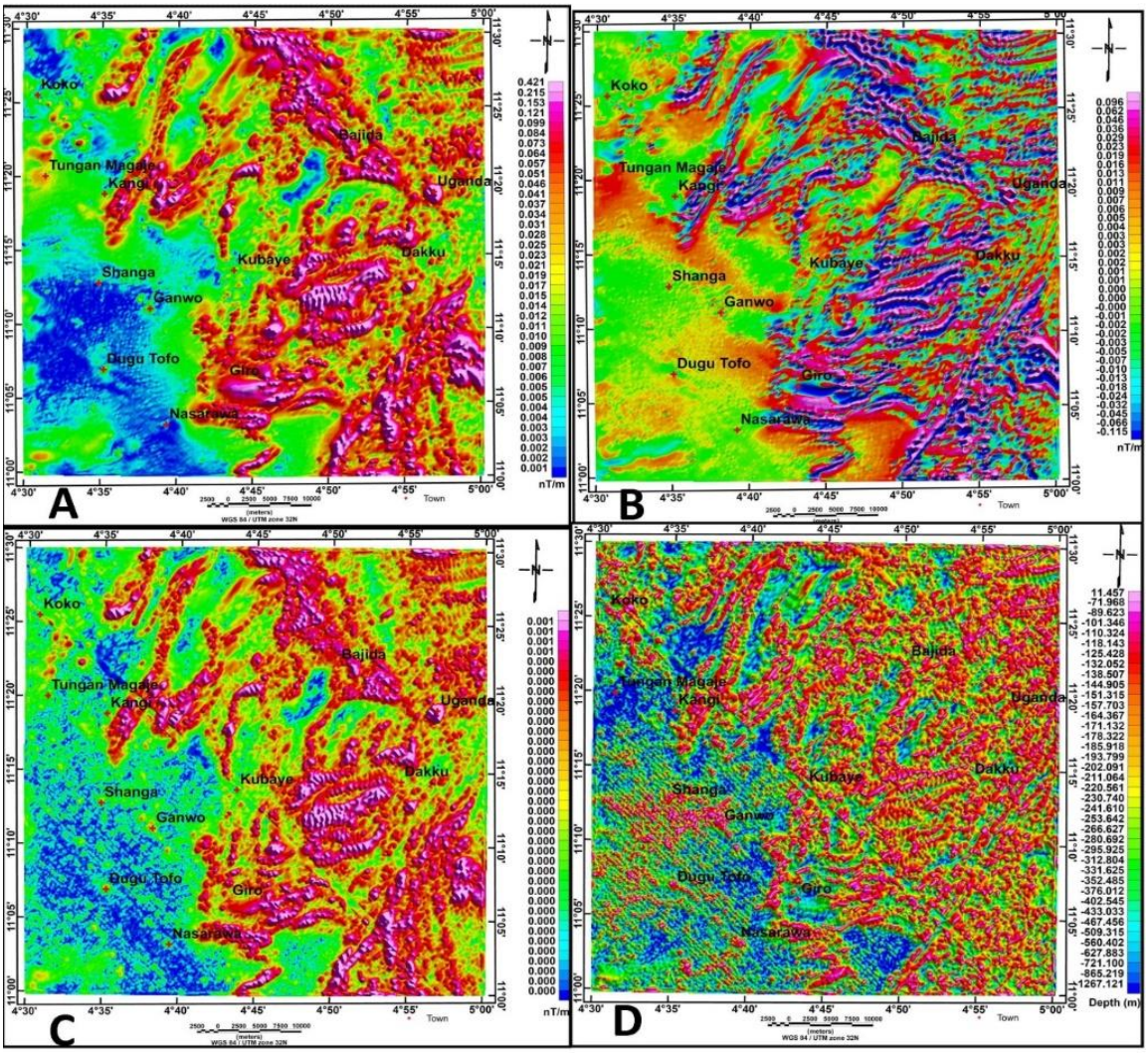

Fig. 13a. AS map b. FVD of Residual anomaly c. AS of FVD map and D. AS Depth

3.5 Estimation of Depth of Minerals Occurrence

The analytic signal depth estimation method was used to estimate the depth of possible occurrence of minerals within the study area. The depths were determined using the analytic signal of residual anomaly (Fig. 13a), the first vertical derivative (Fig. 13b), and the analytic signal of the first vertical derivative (Fig. 13c), while (Fig. 13d) represents the analytic signal depth. From Fig. 13d, the minimum depths for the occurrence of these minerals are from 0 to 11.457 m.

4. CONCLUSION

The use of three source edge detection/interpretation techniques, including analytic signal (AS), first (FVD), and second vertical derivatives have aided in delineating structures within the study area that trend predominantly in the ENE-WSW direction, followed by NE-SW, WNW-ESE, NW-SE, and NNE-SSW directions. The study area has amplitudes ranging from 0.001 nT/m to 0.421 nT/m, and the high analytic signal within the schist has been attributed to intrusions and solidification of mineralisation fluids with structural associations which has enabled the mineralization zones of the area to be delineated. Furthermore, the SVD map revealed mineralization boundaries that coincided with the mineralization zones delineated on the AS map. The mineralization zones delineated have one or more structural lineaments passing through them, confirming that they are responsible for mineralization fluid passage and mineralization hosting within the study area and the analytic signal method revealed a minimum depth of

occurrence for the minerals ranging from 0 to 11.457 m.

COMPETING INTERESTS

Authors have declared that no competing interests exist.

REFERENCES

1. Ajakaiye DE, Hall DH, Ashiekaa JA, Udensi EE. Magnetic anomalies in the Nigerian continental mass based on aeromagnetic surveys. Tectonophysics. 1991;192(1):211-230.
2. Tawey MD, Adetona AA, Alhassan UD, Rafiu AA, Salako KA, Udensi EE. Aeroradiometric data assessment of hydrothermal alteration zones in parts of North Central Nigeria. Asian Journal of Geological Research. 2021;4(2): 1-16.
3. Augie AI, Salako KA, Rafiu AA, Jimoh MO. Geophysical assessment for gold mineralization potential over the southern part of Kebbi State using aeromagnetic data. Geology, Geophysics & Environment. 2022a;48(2): 177-193
4. Amigun JO, Anu AL. Integrated geophysical mapping of structures beneath Ijero – Aramoko Area, Southwestern Nigeria: Implications for control of mineralization. Acta Geologica Sinica. 2013;87:708.
5. Tawey MD, Alhassan DU, Adetona AA, Salako KA, Rafiu AA, Udensi EE. Application of Aeromagnetic Data to Assess the Structures and Solid Mineral Potentials in Part of North Central Nigeria. Journal of Geography, Environment and Earth Science International. 2020a;24(5): 11-29.
   DOI: 10.9734/JGEESI/2020/v24i530223
   Article no. JGEESI.58030. ISSN: 2454-7352.
6. Sani AA, Augie AI, Aku MO. Analysis of gold mineral potentials in Anka schist belt northwestern Nigeria using aeromagnetic data interpretation. J Niger Assoc Math Phy. 2019;52:291–8.
7. Akinlalu AA, Adelusi AO, Olayanju GM, Adiat KAN, Omosuyi GO, Anifowose AYB, Akeredolu BE. Aeromagnetic mapping of basement structures and mineralization characterization of Ilesa Schist Belt, Southwestern Nigeria. J. African Earth Sci. 2018;138:383–391.
   Available:https://doi.org/10.1016/j.jafrearsci.2017.11.033.
8. Uwiduhaye A, Ngaruye JC, Saibi H. Defining potential mineral exploration targets from the interpretation of aeromagnetic data in Western Rwanda. Ore Geol. Rev. 2020;103927.
   Available:https://doi.org/10.1016/j.oregeorev.2020.103927
9. Saibi H, Azizi M, Mogren S. Structural Investigations of Afghanistan Deduced from Remote Sensing and Potential Field Data, Acta Geophysics. 2016;64(4):978–1003.
   DOI: 10.1515/acgeo-2016-0046
10. Azizi M, Saibi H, Cooper GRJ. Mineral and structural mapping of the Aynak-Logar Valley (eastern Afghanistan) from hyperspectral remote sensing data and aeromagnetic data, Arabian Journal of Geosciences. 2015;8(12): 10911-10918.
    DOI: 10.1007/S12517-015-1993-2
11. Akinlalu AA. Radiometric Mapping for The Identification of Hydrothermally Altered Zones Related to Gold Mineralization in Ife–Ilesa Schist Belt, Southwestern Nigeria. Indonesian Journal of Earth Sciences. 2023;3(1):51.
12. Tawey MD, Ibrahim AA, Ehinlaiye AO. Comparative depth to magnetic source analysis of shanga (Sheet 96), North-western Nigeria Using Aeromagnetic Data. African Journal of Environmental Sciences & Renewable Energy. 2023a;12 (1):56-69
13. Joseph A, Sodiq A, Moses A, Bamidele O. Geological structure and hydrothermal alteration mapping for mineral deposit prospectivity using airborne geomagnetic and multispectral data in Zuru Province, northwestern NigeriaThe Egyptian Journal of Remote Sensing and Space Sciences. 2023;26:231-244
14. Kudamnya EA, Andongma WT, Osumeje JO. Hydrothermal mapping of Maru schist belt, north-western Nigeria using remote sensing technique. International Journal of Civil Engineering (IJCE). 2014;3(1):59-66.
15. Augie AI, Salako KA, Rafiu AA, Jimoh MO. geophysical magnetic data analyses of the geological structures with mineralization potentials over the southern part of Kebbi,

NW Nigeria. Mining Science. 2022b;29; 179-203

16. Augie AI, Sani AA. Interpretation of aeromagnetic data for gold mineralisation potential over Kabo and its environs NW Nigeria. Savanna J Basic Appl Sci 2020; 2(2):116–23.
17. Olomo KO, Bayode S, Alagbe SA., Olayanju GM, Olaleye OK. Aeromagnetic Mapping and Radioelement Influence on Mineralogical Composition of Mesothermal Gold Deposit in Part of Ilesha Schist Belt, Southwestern Nigeria, NRIAG Journal of Astronomy and Geophysics. 2022a;11(1): 177-192.
DOI: 10.1080/20909977.2022.2057147
18. Olomoa KO, Bayode S, Alagbe OA, Olayanju GM, Olaley OK. Multifaceted investigation of porphyry cu-au-mo deposit in hydrothermal alteration zones within the gold field of Ilesha schist belt. Malaysian Journal of Geosciences (MJG). 2022b;6 (2),29-37.
DOI:
http://doi.org/10.26480/mjg.02.2022.29.37
19. Taofeeq OL. Integrated aeromagnetic and aeroradiometric data for delineating lithologies, structures, and hydrothermal alteration zones in part of southwestern Nigeria. Arabian Journal of Geosciences. 2020;13:775
Available:https://doi.org/10.1007/s12517-020-05743-7
20. Umaru AO, Kankara AI. Utilizing Landsat-8 sensor operational land image data for hydrothermal alteration mapping within Anka schist belt, northwestern Nigeria. Research Reviews of the Department of Geography, Tourism and Hotel Management 2020;49-2:127-149.
DOI: 10.5937/ZbDght2002127A
21. Umaru AO, Okunlola O, Danbatta UA, Olusegun GO. Litho-structural and hydrothermal alteration mapping for delineation of gold potential zones within Kaiama, northwestern Nigeria, using airborne magnetic and radiometric data. Arabian Journal of Geosciences. 2022; 15:1771
22. Arogundade AB, Awoyemi MO, Ajama OD, Falade SC, Hammed OS, Dasho OA, Adenik CA, Integrated Aeromagnetic and Airborne Radiometric Data for Mapping Potential Areas of Mineralisation Deposits in Parts of Zamfara, Northwest Nigeria. Pure and Applied Geophysics; 2021.
Available:https://doi.org/10.1007/s00024-021-02913-w
23. Roest WR, Verhoefs J, Pilkington M. Magnetic interpretation using 3-D analytic signal Magnetic interpretation using the 3-D analytic signal. Geophysics. 1992;57 (1):116–131.
24. Foss C. Magnetic data Enhancement and Depth Estimation. In H. Gupta (Ed.), Encyclopedia of Earth Sciences Series. 2011:736-746.
25. Nigeria Geological Survey Agency (NGSA). Mineral Resources Map of Nigeria (2006 Ed.). Published by the Authority of the Federal Republic of Nigeria. 2006:1.
26. Obaje NG. Geology and resources of Nigeria 120 lectures notes in Earth Sciences. Springer-Verlag; 2009.
Available:https://doi.org/ 10.1007/978-3-540-92685-6
27. Black R. Precambrian of West Africa. Episodes. 1980;4:3-8.
28. Abba SI. The structure and petrography of alkaline rocks of the Mada Younger Granite Complex, Nigeria. Journal of African Earth Science. 1983;3:107-113.
29. Olayinka AI. Geophysical siting of boreholes in crystalline basement areas of Africa. Journal of African Earth Science. 1992;14:197–207.
30. Gandu AH, Ojo SB, Ajakaiye DE. A gravity study of the Precambrian rocks in the Malumfashi area of Kaduna State, Nigeria. Tectonophysics. 1986;126:181–194.
31. Nigeria Geological Survey Agency (NGSA). Geological Map of Nigeria (2009 Ed.). Published by the Authority of the Federal Republic of Nigeria. 2009;1.
32. Holden EJ, Dentith M, Kovesi P. Towards the automatic analysis of regional aeromagnetic data to identify regions prospective for gold deposits, Computer Geoscience. 2008;34:1505–1513.
Available:https://doi.org/10.1016/j.cageo.2007.08.007
33. Core D, Buckingham A, Belfield S. Detailed structural analysis of magnetic data done quickly and objectively, SGEG Newsletter. 2009;1(2):15–21.
34. Baranov V. A new method for interpretation of aeromagnetic maps: pseudo-gravimetric anomalies. Geophysics. 1957;22:359-383.

35. MacLeod IN, Jones K, Dai TF. 3-D analytic signal in the interpretation of total magnetic field data at low magnetic latitudes. Exploration Geophys. 1993;24(3–4):679–688.

Peer-review history:
The peer review history for this paper can be accessed here:
https://www.sdiarticle5.com/review-history/114779